JOURNAL OF CATALYSIS **159,** 418–426 (1996)
ARTICLE NO. 0105

Reaction Mechanism and Role of the Support in the Partial Oxidation of Methane on Rh/Al_2O_3

Dezheng Wang,[1] Olivier Dewaele, Ann M. De Groote, and Gilbert F. Froment

Laboratorium voor Petrochemische Techniek, Universiteit Gent, Krijgslaan 281, 9000 Gent, Belgium

Received September 14, 1995; revised December 8, 1995; accepted December 11, 1995

The partial oxidation of CH_4 over Rh/Al_2O_3 was studied by means of temporal analysis of products (TAP). CH_4 was found to adsorb dissociatively on reduced metal sites. Oxygen preadsorption decreases the methane adsorption rate. The oxidation products under oxidative conditions are CO_2 and H_2O. The selectivity towards CO and H_2 rises to almost 100% as the conditions become more reductive. Water adsorbed on the support acts as an oxygen source through the inverse spillover of water or hydroxyl onto the Rh particles. A reaction scheme for the partial oxidation of methane is presented and the elementary reactions that give overall steam reforming, CO_2 reforming, and water–gas shift are discussed.

1. INTRODUCTION

Methane conversion is an important area of research because of the need for an efficient utilization of natural gas reserves. Steam reforming of CH_4 is the main process for CH_4 conversion (1, 2). CO_2 (dry) reforming of CH_4 is also a commendable process. Recently, the partial oxidation of CH_4 was shown to be promising with many workers reporting high selectivities to synthesis gas (3–8). Besides, the combustion or total oxidation of CH_4 is an important reaction in automobile exhausts treatment, environmental protection, and energy use (9–11). The above processes are all related and an integrated treatment of their elementary reactions is useful in understanding how they fit into one reaction scheme.

The water–gas shift reaction occurs in the presence of CO, CO_2, H_2 and H_2O. It is sometimes experimentally separated (12, 13) from other reactions with which it can occur, for example CO hydrogenation or Fisher–Tropsch synthesis and CH_4 oxidation. In Fischer–Tropsch synthesis, Rofer-Depoorter (14) argued that it is not useful to separate the water–gas shift reactions conceptually as independent reactions. Instead, they should be analyzed by the actual elementary reactions that lead to overall water–gas shift. In the oxidation of CH_4 it is also useful to identify the subset of elementary reactions that govern the selectivities to CO, CO_2, H_2, and H_2O.

Hickman and Schmidt (15) have presented a model for the partial oxidation of CH_4 using only elementary reactions that are well characterized by surface science techniques. The approach used in the present paper is similar, but it also includes complete oxidation, steam reforming, CO_2 reforming, and water–gas shift.

Rostrup-Nielsen (1, 2) and Grenoble *et al.* (12) have shown that rates in the steam–CO_2 reforming and the water-gas shift reaction, respectively, are significantly influenced by the support. This influence is accounted for in what follows.

2. EXPERIMENTAL

The experiments were performed in a temporal analysis of products (TAP) reactor system from Autoclave Engineers Inc. The reactor has been described by previous workers (16, 17). Essentially, the apparatus is used as a pulse reactor under vacuum with very small pulses of short duration. The residence times are usually less than the reaction, adsorption, and/or desorption times. This allows observations of changes in the peak shapes due to the surface processes. In other words, the response curves of reactants and products give a picture of their sequence in the reaction.

In typical experiments a reactant was pulsed over a reactor bed with pulse sizes of 10^{13} to 10^{15} molecules over 10^{17} to 10^{18} exposed atoms of catalyst, so that the ratio of reactant molecules to exposed atoms was 0.001 to 1%. In this way, changes of the catalyst surface were minimized during the experiments. In addition, the surfaces could maintain their activities for many pulses because water adsorbed on the support cleans the surface of carbon deposited from dissociated CH_4. It was checked that the catalyst did not change with pulses or time by repeating the first train of pulses (a train of pulses was used for signal averaging) at the end of each series. A typical series consisted of trains (10 to 30) of pulses at different *m*/*e* numbers and temperatures.

[1] Permanent address: State Key Laboratory of Catalysis, Dalian Institute of Chemical Physics, Chinese Academy of Sciences, P.O. Box 110, Dalian, 116023, China.

0021-9517/96 $18.00

Individual pulses were observed on a Hewlett-Packard HP 54501 oscilloscope with a memory function to guarantee the absence of systematic variations in the pulse sequence. In other situations transient changes on the surface were studied. For this purpose much larger pulses, containing a number of molecules up to 20% of the exposed Rh atoms, were applied.

The concentrations at the reactor outlet were recorded as a function of time by mass spectrometry using a UTI 100C quadrupole mass spectrometer, a Hewlett-Packard HP 3852A multichannel scaler for signal averaging, and an HP 9000 workstation. The mass spectrometer was tuned to a single mass at a time to avoid dead times resulting from multiplexing. CH_4 was monitored at $m/e = 15$, CO at $m/e = 28$, H_2 at $m/e = 2$, CO_2 at $m/e = 44$, and H_2O at $m/e = 18$. A correction was made for the contribution of CO_2 to $m/e = 28$ from its signal at $m/e = 44$.

The microreactor was a quartz tube with a diameter of 5.6 mm and a length of 42 mm. One end was tapered and polished to give a tight seal when pressed against a Viton O-ring which connected it to the pulse source. The reactor bed consisted of an inert inlet section, a catalyst section, and an inert outlet section. It was kept in place by stainless steel wire screens. The inert sections contained crushed quartz, while the catalyst section consisted of crushed Rh/Al_2O_3 catalyst mixed with SiC particles (to improve thermal conduction). The particle sizes were between 0.25 and 0.50 mm. The reactor temperature was measured by a chromelalumel thermocouple housed in an Inconel sheath (Thermo Electric, 0.16 mm diameter) and positioned in the center of the catalyst bed.

The Rh/Al_2O_3 catalyst had a Rh loading of 0.05 wt% and a BET surface of 153 m^2/g. The Rh particle size was about 3.0 nm (H/Rh = 0.35). This was estimated from the H_2 adsorption capacity assuming cubic crystallites and an H/Rh stoichiometry of 1. The H_2 adsorption capacities were measured on an Altamira AMI-1 unit by pulse chemisorption. Prior to all the experiments, the catalyst was oxidized in an O_2 flow at 873 K for 20 min or 60 min and reduced at 473 K for 20 min before adsorption measurements. These conditions were chosen because EDX analysis showed traces of Ti on the support and complications could arise due to TiO_2 and the SMSI phenomenon (18). Reduction at higher temperatures and/or for longer times lead to a reduced hydrogen adsorption capacity. These capacities were roughly the same for the fresh catalyst and the catalyst from a continuous flow microreactor in which it was used for up to two weeks. There was also no difference in the response curves for a fresh catalyst and a used catalyst.

Blank experiments revealed a strong interaction of water and CO_2 with the support, resulting in broad CO_2 and H_2O responses. During rapid pulsing the H_2O responses could only be detected as an increase of the 18 AMU signal. No interaction of CO and H_2 with the support was detected above 400°C.

3. RESULTS

3.1. Influence of Oxygen and Water on the Partial Oxidation of Methane

Pulsing CH_4 in an oxygen flow resulted in the formation of fully oxygenated products (H_2O and CO_2). No CO and H_2 was detected and the adsorption of CH_4 was found to be slow. The H_2O and CO_2 responses were broadened by strong adsorption on the support. H_2O could not be observed as a separate peak. These responses are not shown here, since the information on the kinetics was lost in the broadening.

When the O_2 flow was stopped and gas-phase O_2 was removed, the adsorption of CH_4 was slow at the beginning of a pulse sequence of CH_4. The adsorption rate then increased with pulsing. After a broad maximum, the adsorption rate decreased again. The curves in Fig. 1 are the response curves to a 90% CH_4–10% Ar pulse sequence over a dehydrated catalyst at 873 K. The catalyst was heated at 1073 K followed by H_2 pulsing to dehydrate the support (20). When the experiment was repeated, but with a catalyst rehydrated with H_2O (6 times the amount of exposed Rh), a broader plateau of high adsorption rate of CH_4 appeared (Fig. 2). An oxygen mass balance showed that the amount of oxygen in the gaseous products was more than the amount of oxygen adsorbed on the Rh. No water was detected in the gas phase. When the support was saturated with water, the plateau was much broader and the high adsorption rate was maintained as a quasi-steady-state. These data show that the water adsorbed on the support is a reactant. The water probably existed as Brønsted acids and bases, but the generic term water is used here.

Figures 1 and 2 show that the CH_4 adsorption was slow during the first pulses after the O_2 flow was stopped. The

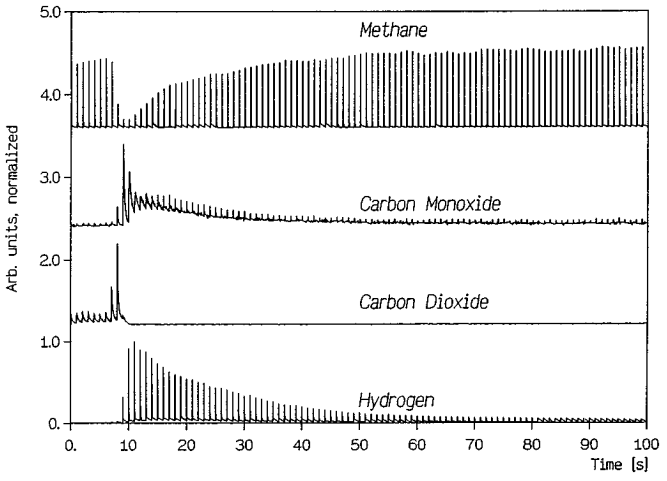

FIG. 1. CH_4, CO, CO_2, and H_2 response curves in a pulsed sequence at 873 K on a catalyst heated at 1073 K for 20 min to remove water from the Al_2O_3 support.

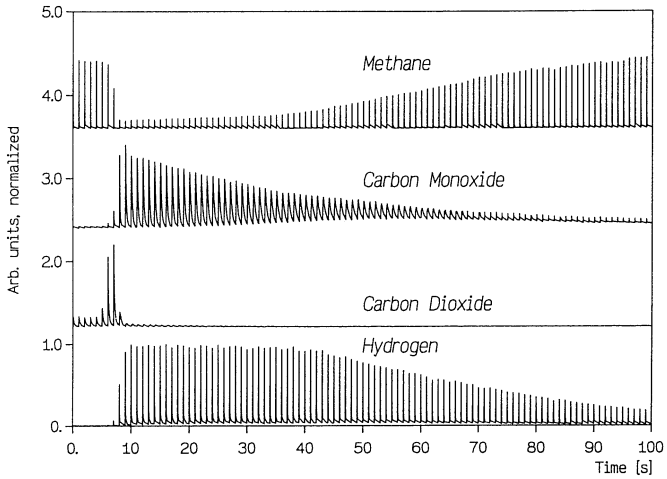

FIG. 2. CH_4, CO, CO_2, and H_2 response curves as a function of the pulsed sequence at 873 K on a catalyst heated at 1073 K for 20 min to remove water from the Al_2O_3 support so that $H_2O/Rh \approx 3$.

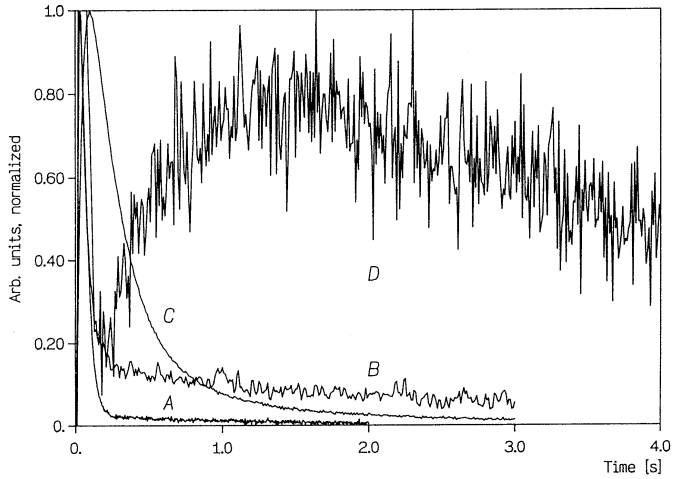

FIG. 3. CO response curves from CH_4–Ar pulses over the catalyst at 873 K. The catalyst had been exposed to a humid atmosphere to saturate the Al_2O_3 support with water and was reduced at 473 K. Curve A is the response almost immediately after the catalyst reached its maximum adsorption rate. Curve B was recorded 100 pulses later. Curve C was recorded immediately after curve B, using a pulse size 10 times bigger. Curve D was recorded 5000 pulses later. The pulse size used for curves A, B, and D was 7×10^{14} CH_4 molecules.

number of these pulses was independent of the amount of water on the support and could be decreased by treating the surface after the evacuation of gaseous O_2 and before the pulse sequence of CH_4. Three different treatments were effective: H_2 pulsing, CO pulsing, and heating under vacuum. Additional experiments showed that a shorter induction period was required for a higher number of H_2 or CO pulses or a longer time of heating under vacuum (19). These treatments are oxygen removing processes. They show that removal of oxygen leads to a faster adsorption of CH_4. A high concentration of adsorbed oxygen inhibits CH_4 adsorption.

Water could not be detected as a pulse because it strongly adsorbed on the support, but it was detected as an increase in the 18 amu signal level during rapid pulsing. It was seen that H_2O was produced when no H_2 was eluted. The selectivity for H_2 and H_2O showed the same behavior as the selectivity for CO and CO_2. The product was CO_2 during the induction period up to when the coverage in oxygen was almost decreased to the level where CH_4 adsorption could readily occur. When the rate of CH_4 adsorption reached its maximum, CO was the main product. H_2 production began just before CH_4 adsorption reached its maximum. This implies that H_2O was produced during the induction period.

3.2. Influence of Water on the Shape of the CO Response

A more detailed inspection of the product response shapes during the pulse sequences provides more information. The shape of the CO_2 response was broadened by adsorption on the support and gives no information on the rate of the CO_2 formation. The shapes of the CO and H_2 response curves on the other hand contain useful information. Figure 3 shows three different shapes of the CO response at various stages in the pulse sequence. A typical feature was the appearance of a tail, which was much broader than the tail of the CO responses to CO pulses in the case of a reduced catalyst and in the absence of water on the support. Curve B shows the emergence of the tail, while curve C shows that the tail arises from a second slower peak. The use of a larger amount of CH_4 in the larger pulse (curve C) lead to a larger tail. This tail became the dominant signal as a second slow peak. The reactant giving rise to the fast peak was used up whereas the amount of a second reactant, which produced the slow peak, remained unchanged.

The second reactant was deduced to be water adsorbed on the support. If it is accepted that the slower response is due to H_2O on the support, then the faster CO response has to be due to preadsorbed oxygen and hydroxyl, since they were the only sources of oxygen. Three reasons form the basis for deducing that water adsorbed on the support was responsible for the slow CO response. (1) The number of pulses during which the slow peak was produced and the peak retention time depended on the amount of water originally present on the support. Curves A to D show the CO responses to CH_4 pulses over a catalyst sample that was progressively depleted of the second reactant. For a drier sample, fewer CH_4 pulses were required to vary the shape of the CO response from A to D than for more hydrated samples. (2) The response time of the slow CO peak was temperature dependent. For a comparable amount of H_2O on the support, the CO responses could have the shape of curve B at 873 K and of curve D at 773 K. H_2O migration over the support can be expected to be quite temperature dependent, but such a large activation energy is not expected for the reaction of adsorbed oxygen and carbon

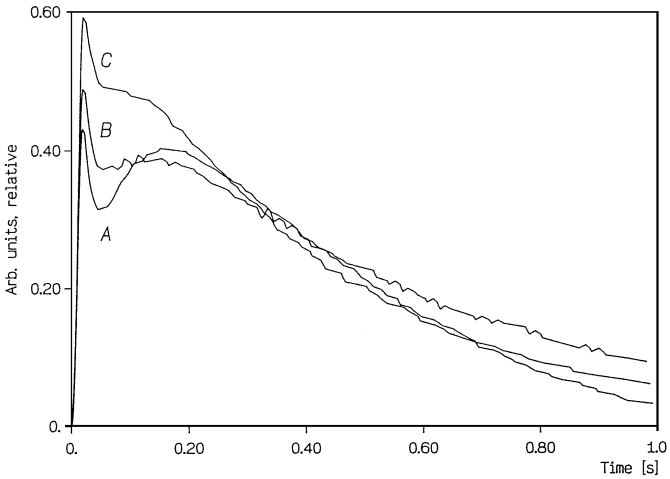

FIG. 4. The CO response curves due to pulsed CH_4 as a function of pulsing frequency. Curve A was the response from 1 CH_4 pulse/sec, curve B was the response from 1 CH_4 pulse per 2.5 seconds, and curve C was the response from 1 CH_4 pulse per 5 seconds.

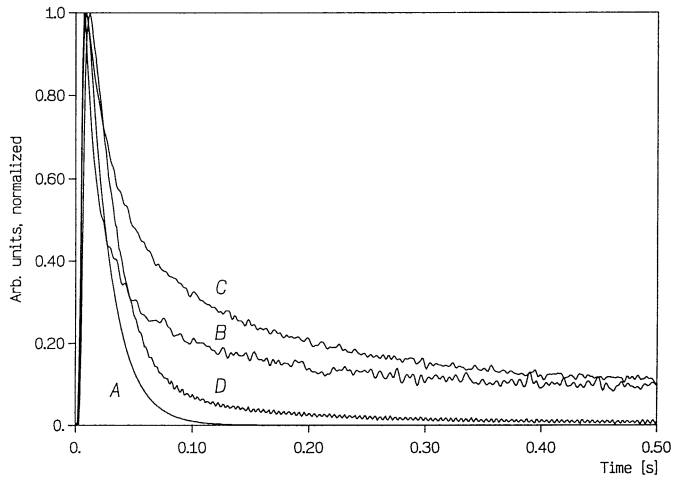

FIG. 5. H_2 response curves from H_2–He pulses over the catalyst at 673 K. Curve A is a simulated curve to show the H_2 response when desorption is fast and adsorption does not influence the pulse shape. Curve B is the response over a catalyst that had been heated at 973 K for 30 min to remove some water from the Al_2O_3 support. Curve C is from a catalyst that had been exposed to a humid atmosphere to saturate the Al_2O_3 support with water and was reduced at 473 K. Curve D shows the He internal standard.

species. (3) A third reason is given in Fig. 4. The figure shows the CO responses corresponding to those of curves B and C in Fig. 3, but with an intermediate CH_4 pulse size, resulting in the appearance of both peaks. The curves are given as a function of the pulsing frequency. The slower peak became slower as the pulsing frequency was increased. A possible interpretation is that the amount of water adsorbed on the support in the immediate vicinity of the metal particles was smaller for a higher pulsing frequency, resulting in a slower migration of H_2O onto the rhodium particles.

3.3. Influence of Water on the Shape of the Hydrogen Response

Figures 5 and 6 show the H_2 response curves when H_2 was pulsed over the catalyst with supports loaded with different amounts of water. In Fig. 5, a comparison of curves B and C with curve A shows that responses B and C were broadened. The broadening depended on the amount of water on the Al_2O_3 support. There was more broadening for higher water loadings on the support. Figure 6 shows that the tail increased with temperature. This means that assigning the tail to adsorption–desorption on Rh would imply that H_2 adsorption was activated, since the fraction of the H_2 pulse in the tail increases with temperature. There is good evidence that H_2 adsorption on Rh is not activated (21). Therefore, the tail was assigned to H_2 evolved during the dissociative adsorption of H_2O which migrated from the support onto the Rh. It was activated because H_2O diffusion or desorption over Al_2O_3 is known to be activated (20).

Further evidence of the role of water adsorbed on the support can be seen in Fig. 7, which shows the response curves of H_2 to CH_4 pulses at 873 K over a dehydrated and a hydrated catalyst. The broad response in curve A was similarly assigned to water adsorbed on the support. This broad response also implied prior adsorbed oxygen: preadsorbed oxygen removed hydrogen from CH_4 dissociation, by its oxidation to $-OH$ and H_2O, and resulted in a smaller H_2 peak from CH_4 dissociation. When there was H_2O on the support, adsorbed oxygen was replenished from the dissociative adsorption of water from the support, leading to the

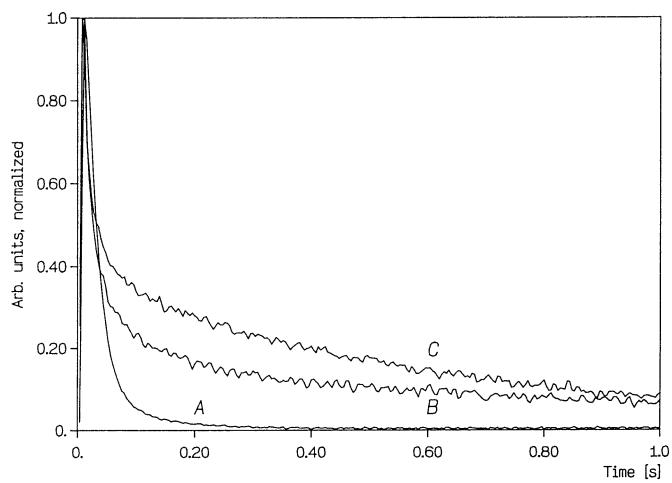

FIG. 6. H_2 response curves from H_2–He pulses over the catalyst at (B) 773 and (C) 973 K. Curve A is the He internal standard. The catalyst had been exposed to a humid atmosphere to saturate the Al_2O_3 support with water and reduced at 473 K, and was heated at 973 K for 30 min to remove some water from the Al_2O_3 support before collecting the data for curve B. Data for curve C was taken immediately after temperature equilibration after curve B.

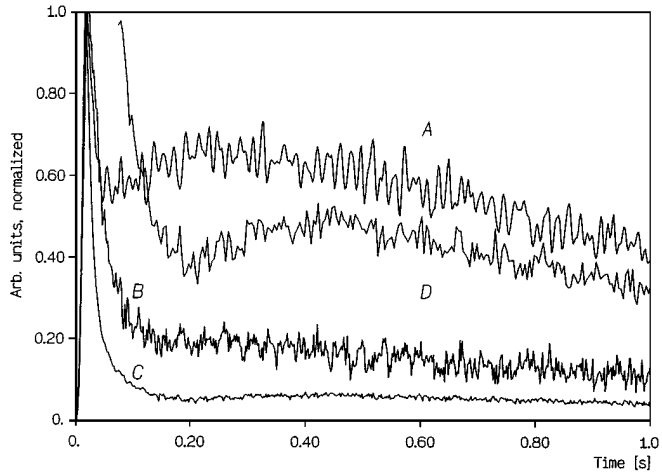

FIG. 7. H_2 response curves from CH_4—Ar pulses over the catalyst at 873 K. The catalyst had been exposed to a humid atmosphere to saturate the Al_2O_3 support with water, and was reduced at 473 K. Curve A is the response almost immediately after the catalyst reached its maximum adsorption rate. Curve B was recorded 100 pulses later. Curve C was recorded 5000 pulses later. Curve D is an expanded plot of curve C. The pulse size used was 7×10^{14} CH_4 molecules.

broad tail in the H_2 response curve. This tail decreased with time, due to heating which dehydrates the catalyst, and also with pulsing CH_4 which removes oxygen containing species by reaction. The tail was not evident when the catalyst was well dehydrated before pulsing CH_4.

3.4. Influence of Water on the Conversion of CO

Figure 8 provides more evidence of an inverse spillover of adsorbed H_2O from the support. In this case, CO was pulsed over a hydrated catalyst and H_2 was evolved. CO_2 was also produced, but could only be observed as a pulse response above 873 K because of its adsorption and slow desorption from the support. H_2 production was seen in the temperature range of 723 to 1023 K. The intensities of the response curves dependent on the amount of H_2O adsorbed on the support and on the temperature. Larger amounts of H_2O or higher temperatures resulted in a higher conversion of CO. When the catalyst was dehydrated, no CO conversion was detected. It is unlikely that CO_2 was produced by disproportionation of CO to surface carbon and CO_2 (the Boudouard reaction) because there was no loss in activity for CO conversion when H_2O was present on the support. Also, the rate of the Boudouard reaction is not expected to strongly depend on the amount of adsorbed H_2O on the support or to show a strong temperature dependence in the range from 723 to 1023 K. Figure 8 compares the H_2 responses from H_2 pulses (curve B) and CO pulses (curve C). The left shoulder in curve C contains no information: it was assumed to be a TAP "push-through": the pulsed molecules collide with molecules still present at the inlet of the reactor during the pulse time, producing a fast peak. Ignoring the left shoulder in curve C, curve C is quite similar to the tail in curve B. Consistent with the above interpretation, it was assigned to spillover H_2O. Spillover H_2O from the support dissociated on the metal leading to adsorbed oxygen and hydroxyl and desorbed H_2. Adsorbed CO reduced the surface when it was oxidized by the adsorbed oxygen or hydroxyl. Figure 9 shows the CO reactant pulses and the CO_2 product pulses as a function of the amount of H_2O on the support. The sharpening of the reactant pulse reflects a higher conversion, the sharpening of the product response a faster oxidation. There was more conversion of CO and

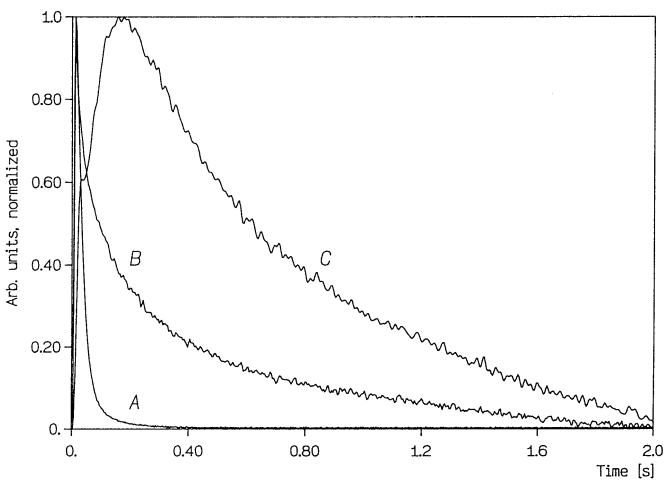

FIG. 8. Curve A is the He internal standard and curve B is the response curves from H_2–He pulses over the catalyst at 773 K. The catalyst had been exposed to a humid atmosphere to saturate the Al_2O_3 support with water, and was reduced at 473 K. Curve C is the H_2 response curve from CO–Ar pulses at 773 K.

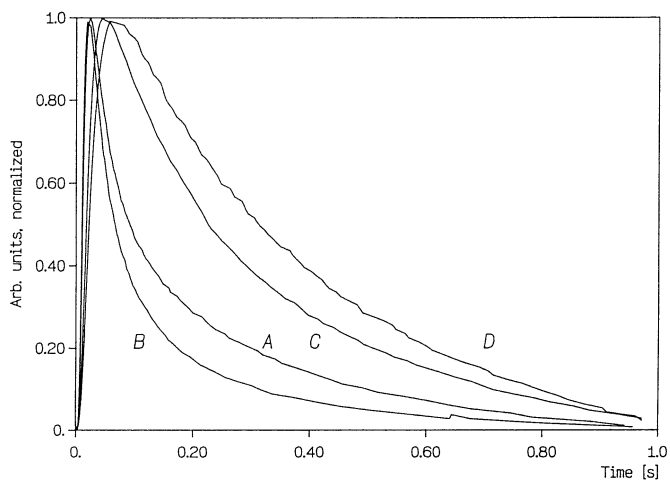

FIG. 9. The CO and CO_2 response curves from CO pulses as a function of the amount of H_2O on the support. Curves A and C are from a catalyst loaded with 1×10^{17} molecules of H_2O after it was first dehydrated. Curves B and D are from a catalyst containing 3 times as much H_2O.

faster oxidation to CO_2 when there was more H_2O on the support.

4. DISCUSSION

4.1. Reaction Mechanism

Based on the above results and literature information the following mechanism is proposed for the partial oxidation of methane to synthesis gas over an Rh/Al_2O_3-catalyst.

Events on Rh-sites:

adsorption steps and dissociation of methane:

$$O_2 + 2l_1 \rightleftharpoons 2O\text{-}l_1 \quad [1]$$

$$CH_4 + l_1 \rightleftharpoons CH_4\text{-}l_1 \quad [2]$$

$$CH_4\text{-}l_1 + l_1 \rightleftharpoons CH_3\text{-}l_1 + H\text{-}l_1 \quad [3]$$

$$CH_3\text{-}l_1 + l_1 \rightleftharpoons CH_2\text{-}l_1 + H\text{-}l_1 \quad [4]$$

$$CH_2\text{-}l_1 + l_1 \rightleftharpoons CH\text{-}l_1 + H\text{-}l_1 \quad [5]$$

$$CH\text{-}l_1 + l_1 \rightleftharpoons C\text{-}l_1 + H\text{-}l_1 \quad [6]$$

surface reaction steps

$$O\text{-}l_1 + H\text{-}l_1 \rightleftharpoons OH\text{-}l_1 + l_1 \quad [7]$$

$$C\text{-}l_1 + O\text{-}l_1 \rightleftharpoons CO\text{-}l_1 + l_1 \quad [8]$$

$$C\text{-}l_1 + OH\text{-}l_1 \rightleftharpoons COH\text{-}l_1 + l_1 \quad [9]$$

$$COH\text{-}l_1 + l_1 \rightleftharpoons CO\text{-}l_1 + H\text{-}l_1 \quad [10]$$

$$CO\text{-}l_1 + O\text{-}l_1 \rightleftharpoons CO_2\text{-}l_1 + l_1 \quad [11]$$

$$CO\text{-}l_1 + OH\text{-}l_1 \rightleftharpoons CO_2\text{-}l_1 + H\text{-}l_1 \quad [12]$$

$$CH_x\text{-}l_1 + OH\text{-}l_1 \rightleftharpoons CH_{x+1}O\text{-}l_1 + l_1 \quad [13]$$

$$CH_x\text{-}l_1 + O\text{-}l_1 \rightleftharpoons CH_xO\text{-}l_1 + l_1 \quad [14]$$

$$CH_xO\text{-}l_1 + l_1 \rightleftharpoons CO\text{-}l_1 + xH\text{-}l_1 \quad [15]$$

$$OH\text{-}l_1 + H\text{-}l_1 \rightleftharpoons H_2O\text{-}l_1 + l_1 \quad [16]$$

$$2OH\text{-}l_1 \rightleftharpoons H_2O\text{-}l_1 + O\text{-}l_1 \quad [17]$$

desorption steps

$$CO\text{-}l_1 \rightleftharpoons CO + l_1 \quad [18]$$

$$2H\text{-}l_1 \rightleftharpoons H_2 + 2l_1 \quad [19]$$

$$CO_2\text{-}l_1 \rightleftharpoons CO_2 + l_1 \quad [20]$$

$$H_2O\text{-}l_1 \rightleftharpoons H_2O + l_1. \quad [21]$$

Events on Al_2O_3-sites:

$$H_2O + l_2\text{-}O\text{-}l_2 \rightleftharpoons OH\text{-}l_2 + H\text{-}O\text{-}l_2 \quad [22]$$

$$OH\text{-}l_2 + H\text{-}O\text{-}l_2 \rightleftharpoons O\text{-}l_2 + H_2O\text{-}l_2. \quad [23]$$

Inverse spillover from the support to the metal surface:

$$H_2O\text{-}l_2 + l_1 \rightleftharpoons H_2O\text{-}l_1 + l_2. \quad [24]$$

In the above mechanism the adsorption sites l_1 and l_2 represent, respectively, an Rh-site and an Al_2O_3-site. Oxygen adsorbs dissociatively on the Rh-surface (1). The adsorption of CH_4 on Rh is a sequence of C–H cleavages ([2–6]), which are very fast. Both O-l_1 and OH-l_1 may result from H_2O dissociation ([16, 17]). Adsorbed oxygen and hydroxyl are also produced by inverse spillover of H_2O from the support at low concentrations of O-l_1. A nucleophilic attack of an adsorbed hydroxyl group on an adsorbed CO molecule [12] and on the CH_x species [13] is also included. It is likely that reaction step [12] is of importance only when the concentration of hydroxyl groups is high or when there is a considerable amount of water on the support. Reaction steps [2–4], [11], [14] for $x = 2$, [15] for $x = 1$, and [18–20] also occur in the mechanism proposed by Xu and Froment (26) for the steam reforming of methane on a Ni-catalyst. Hickman and Schmidt (15) proposed a shorter but analogous mechanism for the partial oxidation of methane over alumina foam monoliths coated with a high loading of Rh or Pt.

The partial oxidation of CH_4 on Rh/Al_2O_3 was also studied by Buyeskaya *et al.* (34). This work provides an important corroboration for experimental data. Where a comparison of experimental results is possible, the agreement in the shapes of the response curves and reaction selectivity are very good, even though the interpretations are quite different.

4.2. Dissociation of Methane

The results suggest that metallic Rh is the active surface for methane dissociation. The active surface may also be covered partially with adsorbed oxygen or adsorbed hydroxyl. Indeed, the support strongly retains H_2O and this leads to adsorbed oxygen as well as adsorbed hydroxyl from inverse spillover after reduction of the catalyst. The O-l_1 concentration can be very low when the support is completely dehydrated by heating under vacuum or by the oxidation of many CH_4 pulses, resulting in a very broad CO response. Under these conditions the surface is still active, so that the CH_4 dissociation probably proceeds on the metal. Also, the rates of CH_4 adsorption and CO and CO_2 production vary gradually from reaction on an oxygen saturated surface or a H_2O saturated support to reaction on a surface that consists of almost bare metal. This continuity is the basis for the assumption that the reduced surface is the active site for CH_4 dissociation, even when the oxygen coverage is high. This is consistent with the conclusion of the review on the mechanism of CH_4 adsorption on metals by Haller and Coulson (21).

Garbowski *et al.* (11) and Zum Mallen *et al.* (31) suggested that C–H cleavage occurs through adsorption on ad-

sorbed oxygen. This can explain why CH_4 reactions can still take place on a surface saturated with oxygen, but it contradicts observations indicating that adsorbed oxygen inhibits CH_4-adsorption (9). This is shown in Figs. 1 and 2, where the removal of oxygen results in accelerated methane adsorption and gives rise to the question of how CH_4 adsorption can take place on an oxygen saturated surface. CH_4 dissociation can occur on metal sites even on an oxygen saturated surface because oxygen saturation above 650 K does not mean full coverage of all metal sites. There may be small patches of vacant Rh sites. In this case the oxidation follows a dual site mechanism, in agreement with most of the literature in this field (1, 4, 5, 7–9).

4.3. The Primary Products

When the concentration of O-l_1 is high, i.e., when gas-phase oxygen is present or just after the removal of the gas-phase oxygen, the products are CO_2 and H_2O. For low concentrations of O-l_1, when CH_4-adsorption has reached its maximum value in a pulsed sequence, the products are CO and H_2.

These conclusions are in agreement with the work of Prettre *et al.* (3), Green *et al.* (14), and Lunsford *et al.* (5), according to whom the partial oxidation of methane into synthesis gas consists of the total combustion of a fraction of the methane into CO_2 and H_2O, followed by steam reforming and CO_2-reforming of the remaining methane, accompanied by the water–gas shift reaction. The absence of H_2O and CO_2 reforming simultaneous with the total combustion can be explained by the rapid oxidation of adsorbed H_2 and CO at high oxygen concentrations. In that case the concentration of adsorbed oxygen O-l_1 is so high that CO and H_2 cannot desorb without oxidation. This corresponds to the general observation that CO_2 and H_2O are the main products under oxygen-rich conditions (9, 11, 25), while CO and H_2 are only observed at higher CH_4/O_2-ratios (4, 5, 8, 10).

According to Schmidt *et al.* (7, 15, 33) and to Peters (6) CO and H_2, and not CO_2 and H_2O, are the primary products in the partial oxidation of methane at temperatures above 1000 K and very high space velocities. In some pulse experiments a region of fast CO-production is observed which is probably due to oxidation by previously adsorbed oxygen (viz. the fast CO peak in Figs. 3 and 4). In all experiments some H_2O is present on the support from the removal of adsorbed oxygen with the first pulses during the period of slow methane adsorption, as shown in Figs. 1 and 2. This water can be removed by heating the support after these pulses. Subsequent CH_4-pulses also lead to fast CO and H_2 production and these are primary products (in the absence of water). The adsorption rate of CH_4 decreases rapidly because of poisoning by adsorbed CH_x species and there is only a narrow range of O-l_1 concentrations for which CO is formed as a primary oxidation product rather than as a product of steam reforming.

Therefore, a distinction can be made between two possible cases, one where the partial oxidation of CH_4 into synthesis gas is a primary reaction and one where total combustion of CH_4 into CO_2 and H_2O is followed by steam and CO_2-reforming. When the concentration of O-l_1 is low because of low partial pressures of oxygen, short residence times, or fast desorption of oxygen at high temperatures, the desorption of CO and H_2 is favored over their oxidation and only small amounts of CO_2 and H_2O are produced. In the case of high O-l_1 concentrations the initial products are CO_2 and H_2O. When most of the oxygen is consumed, a low oxygen coverage is maintained at temperatures above 1000 K, since methane adsorption is faster than the dissociative adsorption of H_2O and CO_2, so that CO and H_2 are the secondary products.

In some experiments of the present work it was shown that CO may elute quite late. Since the elution time of CO gradually increases when the catalyst is continuously heated under vacuum, it is assumed that the elution time is a measure for the rate of inverse spillover or surface migration over the support, so that it can be concluded that CH_4 adsorption is faster than oxygen and hydroxyl adsorption from inverse spillover. This also reflects that CO-l_1 is likely to desorb before nucleophilic attack by OH-l_1 at low concentration of O-l_1.

4.4. Inverse Spillover in Steam Reforming

An important reaction step in the mechanism is the inverse spillover of water. In Figs. 1–7, three features are ascribed to the spillover of water on the support. (1) A plateau was observed, during which the rate of CH_4 adsorption was fast. The length of this plateau depended on the amount of H_2O adsorbed on the support. (2) A slow peak in the CO response was observed. This peak appeared for many pulses and broadened much slower as a function of the number of pulses in the presence of H_2O on the support. (3) There could be a tail in the H_2 response curves from both CH_4 and H_2 pulses. The tail in the H_2 responses and the slow CO responses strongly depended on the temperature, particularly in the temperature range between 723 and 1023 K.

The above features show that water adsorbed on the Al_2O_3 support is a reactant. The partial pressure of water in the gas phase did not significantly change with the water loading. This indicates that an inverse spillover mechanism from the support to the metal is operative, rather than desorption–readsorption. All three phenomena occured in the same temperature range (723–1023 K) and each phenomenon is more pronounced at higher temperatures. This is evidence for a process of inverse spillover. H_2O desorption from Al_2O_3 is activated and loss of H_2O from the support is rapid above 1023 K (21). It is possible that an adsorbed precursor for desorption is mobile between 723 and 1023 K.

An inverse spillover of H_2O was also suggested by Rostrup-Nielsen (1) as a source of H_2O for the metal to explain the differences in the steam reforming rates on catalysts with different supports. This does not imply that H_2O adsorbed on the metal only results from inverse spillover of H_2O from the support. Besides inverse spillover, Rostrup-Nielsen also reported a desorption–readsorption mechanism on the metal.

The mechanism for H_2O adsorption on the metal depends upon that for H_2O desorption from the support. When adsorption on the support occurs through a chemisorbed H_2O molecule which is mobile over the Al_2O_3 surface, H_2O adsorbed on the metal mainly comes from inverse spillover, especially when the partial pressure of H_2O in the bulk gas phase is low or at temperatures where desorption from the support is slow.

It may be assumed that H_2O adsorbs as Brønsted acids and bases. At sufficiently high temperatures, but at which desorption is still slow, a mobile intermediate can be formed from the recombination of these acids and bases. This intermediate would be hydrogen bonded to the support and capable of migrating to the Rh surface. The following equilibrium was suggested by Peri (21):

$$2OH^- \rightleftharpoons H_2O + O^{2-}.$$

Peri (21) also showed that almost complete dehydration of Al_2O_3 takes place above 1073 K. In the present work the desorption of H_2O from the support is found to be fast at temperatures above 1023 K. Inverse spillover is observed in the temperature range between 723 and 1023 K. Based on the mechanism presented here, it is likely that inverse spillover becomes more important when the support is highly hydrated and the partial pressure of H_2O in the bulk gas phase is too low to result in a significant adsorption rate on the Rh.

The inverse spillover from the support is a step in the overall steam reforming reaction and is a source of H_2O for the Rh sites on which dissociation occurs. The resulting adsorbed oxygen and hydroxyl then oxidize the adsorbed CH_x species.

4.5. Mechanism of the Water–Gas Shift Reaction

Several reaction schemes were reported in the literature for the water–gas shift reaction. Grenoble *et al.* (12) proposed a mechanism consisting of a spillover of CO to the support, formate formation on the support, formate migration, and dissociation of the formate on the metal. These bifunctional features are used to explain the differences in the rate of the WGS-reaction on catalysts with different supports. Amenomiya (27) also reported the existence of formate on Al_2O_3. Rofer-DePoorter (14) suggested that this mechanism may occur at temperatures below 573 K. At higher temperatures the desorption of CO from the metal and the dissociation of formate on the support are fast and a different mechanism is more likely to occur on the metal.

For the temperature range covered in the partial oxidation of CH_4 the proposed steps in the overall water–gas shift reaction are oxygen transfer from H_2O or CO_2 to the catalyst and from the catalyst to CO or H_2, as suggested by other workers (13, 14, 28) for higher temperatures. The reaction pathway on Rh/Al_2O_3 is similar, but includes an inverse spillover of H_2O. There is strong evidence that the support is not inert (12) and the inverse spillover steps attribute an active role to the support, depending upon its ability to adsorb H_2O and allow surface diffusion of H_2O.

Most of the reaction steps used in the reaction pathway of the present paper are well accepted in the literature and are not discussed here. The inverse spillover of H_2O from the support is already discussed in Section 4.4. The other additional step is a nucleophilic attack of adsorbed hydroxyl on adsorbed CO [12]. This step is based upon the observation that CO_2 is an important product at high O-l_1 concentration on a reduced catalyst when the support is saturated with H_2O. This proves that adsorbed H_2O is the reactant. Thiel and Madey (22), Padowitz and Sibener (23), and Zum Mallen *et al.* (24) showed that an equilibrium exists between adsorbed OH and hydrogen and oxygen; OH-l_1 is also a product of adsorbed H_2O. This step was previously proposed by Rofer-Depoorter (14, 29) on the basis of the homogeneous water–gas shift reaction.

4.6. Nucleophilic Attack of Adsorbed Hydroxyl on CH_x Species

The nucleophilic attack of OH-l_1 on adsorbed CH_x species [13] is similar to that discussed in Section 4.5. The first occurs at low concentrations of O-l_1 as well as at high concentrations, since CH_x species cannot desorb by themselves, unlike CO. This step [13] was used by Joyner *et al.* (30) to explain the role of H_2O in CO hydrogenation over Rh in oxygenate synthesis and has been experimentally verified in homogeneous catalysis (31). Menon *et al.* (32) and Oh *et al.* (10) discussed the existence of a formaldehyde-type intermediate.

The tail in the H_2 responses on CH_4 pulses may also indicate that CH_4 is not completely dehydrogenated before the oxidative attack occurs. For the time being it is not possible to distinguish between H_2 resulting from H_2O dissociation and H_2 produced from the decomposition of oxygenated hydrocarbon species. By comparing the elution times of the CO and H_2 responses it seems reasonable to assign H_2 in the peak to hydrogen cleaved before oxidation of adsorbed CH_x and part of the H_2 in the tail to hydrogen cleaved after the decomposition of the oxidized hydrocarbon species. These observations point towards intermediates like formaldehyde, formate, or hydroxylcarbonyl.

Since there was no tail in the H_2 response from an active and well-dehydrated catalyst and since the

hydrogen/carbon ratio was about 4/1, the reaction intermediate in that case is most likely close to a surface carbide. In some experiments, though, a 30-amu response was observed when CH_4 was pulsed over a catalyst that had lost much of its activity. Therefore, the mechanism in the present paper allows for both surface carbide and formaldehyde intermediates. The type of the intermediate depends upon the oxidizing agent and the degree of hydrogen loss of the CH_x species before the oxidation step.

5. CONCLUSION

The products and the kinetics of the oxidation of CH_4 depend on the concentration of adsorbed oxygen. At high concentrations of adsorbed oxygen the products are H_2O and CO_2 and methane adsorption is inhibited. At low concentrations of adsorbed oxygen CH_4 adsorption is fast and occurs on metal sites. In that case the products are CO and H_2.

CO_2 is formed from adsorbed CO by fast oxidation with adsorbed oxygen or by the nucleophilic attack of adsorbed hydroxyl. H_2O is formed from the rapid reduction by hydrogen of adsorbed hydroxyl and adsorbed oxygen. CO is produced from CH_x through the oxidation by means of adsorbed oxygen or by the nucleophilic attack by adsorbed hydroxyl. CO is also formed in the dissociation of CO_2. Hydrogen is generated from CH_4- and H_2O-dissociation.

Water adsorbed on the support is shown to spill over to the metal phase.

ACKNOWLEDGMENTS

Dezheng Wang thanks the Belgian National Fonds voor Wetenschappelijk Onderzoek for a fellowship within their Belgian-Sino cooperation program, and the Dalian Institute of Chemical Physics and the Chinese Academy of Sciences for granting a leave of absence. Olivier Dewaele also thanks the Belgian National Fonds voor Wetenschappelijk Onderzoek for this Research Fellowship. We thank P. G. Menon for help with the measurements of hydrogen adsorption capacity and Marie-Francoise Reyniers and Tom Degres for their assistance in some experiments.

REFERENCES

1. Rostrup-Nielsen, J. R., *in* "Catalysis. Science and Technology" (J. R. Anderson and M. Boudart, Eds.) Vol. 5, p.1. Springer, Berlin, 1984.
2. Rostrup-Nielsen, J. R., and Bak-Hansen, J. H., *J. Catal.* **144**, 38 (1993).
3. Pettre, M., Eichner, C. H., and Perrin, H., *Trans. Faraday Soc.* **23**, 257 (1946).
4. Ashcroft, A. T., Cheetham, A. K., Foord, J. S., Green, M. L. H., Grey, C. P., Murrell, A. J., and Vernon, P. D. F., *Nature* **344**, 319 (1990).
5. Dissanayake, D., Rosynek, M. P., Kharas, K. C. C., and Lunsford, J. H., *J. Catal.* **132**, 117 (1991).
6. Peters, K., Rudolf, M., and Voetter, H., *Brennstoff-Chem.* **36**, 257 (1955).
7. Torniainen, P. M., Chu, X., and Schmidt, L. D., *J. Catal.* **146**, 1 (1994).
8. Choudhary, V. R., Sausane, S. D., and Mamman, A. S., *Appl. Catal. A* **40**, L1 (1992).
9. Burch, R., and Loader, P. K., *Appl. Catal. A* **122**, 169 (1995).
10. Oh, S. H., Mitchell, P. J., and Siewart, R. M., *J. Catal.* **132**, 287 (1991).
11. Garbowski, E., Feumi-Jantou, C., Mouaddib, N., and Primet, M., *Appl. Catal. A* **109**, 277 (1994).
12. Grenoble, D. C., Estadt, M. M., and Ollis, D. F., *J. Catal.* **64**, 90 (1981).
13. Rhodes, C., Hutchings, G. J., and Ward, A. M., *Catal. Today* **23**, 43 (1995).
14. Rofer-DePoorter, C. K., *in* "Catalytic Conversions of Synthesis Gas and Alcohols to Chemicals," (R. G. Herman, Ed.), p. 97, Plenum, New York, 1984.
15. Hickman, D. A., and Schmidt, L. D., *AIChE. J.* **39**, 1164 (1993).
16. (a) Lafyatis, D. S., Froment, G. F., Pasau-Claerbout, A., and Derouane, E., *J. Catal.* **147**, 552 (1994); (b) Lafyatis, D. S., Creten, G., and Froment, G. F., *Appl. Catal. A* **120**, 85 (1994).
17. Gleaves, J. T., Ebner, J. R., and Kuechler, T. C., *Catal. Rev. Sci. Engr.* **30**, 43 (1989).
18. Haller, G. L., and Resasco, D. E., *Adv. Catal.* **36**, 183 (1989).
19. Dewaele, O., Ir. thesis, Universiteit Gent, 1994.
20. Peri, J. B., *J. Phys. Chem.* **69**, 211 (1965).
21. Haller, G. L., and Coulston, G. W., *in* "Catalysis. Science and Technology" (J. R. Anderson and M. Boudart, Eds.), Vol. 9, p. 131, Springer, Berlin, 1991.
22. Thiel, P. A., and Madey, T. E., *Surf. Sci. Rept.* **7**, 297 (1987).
23. Padowitz, D. F., and Sibener, S. J., *Surf. Sci.* **254**, 125 (1991).
24. Zum Mallen, M. P., Williams, W. R., and Schmidt, L. D., *J. Phys. Chem.* **97**, 625 (1993).
25. Cullis, C. F., and Willatt, B. M., *J. Catal.* **83**, 267 (1983).
26. Xu, J., and Froment, G. F., *AIChE J.* **35**, 88 (1989).
27. (a) Amenomiya, Y., *J. Catal.* **55**, 205 (1978); (b) Amenomiya, Y., and Pleizier, G., *J. Catal.* **76**, 345 (1982).
28. Lloyd, L., Ridler, D. E., and Twigg, M. V., *in* "Catalyst Handbook," (M. V. Twigg, Ed.), 2nd ed., p. 283. Wolfe, London, 1989.
29. Rofer-DePoorter, C. K., *Chem. Rev.* **81**, 447 (1981).
30. Johnston, P., and Joyner, R. W., *in* "Proceedings, 10th International Congress on Catalysis, Budapest, 1992" (L. Guczi, F Solymosi, and P. Tetenyi, Eds.), Vol. A., p. 165. Elsevier, Amsterdam, 1992.
31. Crabtree, R. H., "Organic Chemistry of Transition Metals." Wiley, New York, 1988.
32. Menon, P. G., Dedeken, J., and Froment, G. F., *J. Catal.* **95**, 313 (1985).
33. Huff, M., and Schmidt, L. D., *J. Phys. Chem.* **97**, 815 (1993).
34. Buyevskaya, O. V., Wolf, D., and Baerns, M., *Catal. Lett.* **29**, 249 (1994).